

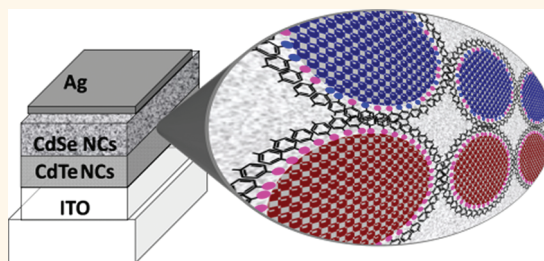
Combining Ligand-Induced Quantum-Confined Stark Effect with Type II Heterojunction Bilayer Structure in CdTe and CdSe Nanocrystal-Based Solar Cells

Nir Yaacobi-Gross,[†] Natalia Garphunkin,[†] Olga Solomeshch,[†] Aleksandar Vaneski,[‡] Andrei S. Sussha,[‡] Andrey L. Rogach,[‡] and Nir Tessler^{†,*}

[†]Zisapel Nano-electronics Centre, Department of Electrical Engineering, Technion—Israel Institute of Technology, Technion City, Haifa 32000, Israel and [‡]Department of Physics and Materials Science & Centre for Functional Photonics (CFP), City University of Hong Kong, Hong Kong SAR

Semiconducting nanocrystals (NCs) are promising materials for various optoelectronic applications.^{1–3} The quantum size effect, which allows energy level tuning, makes NCs especially attractive for photovoltaic (PV) devices, where the NC absorption could be tailored to allow maximum overlap with the solar spectrum.⁴ Another key advantage of NCs is their compatibility with various solvents, which allow low-cost and large-area fabrication. Since the canonical publication of the “hot injection” synthetic technique by Murray *et al.*,⁵ many modifications of this organics-based procedure have been suggested in order to improve the size and shape control of the NCs as well as to simplify the experimental protocol.⁶ One important development was the introduction of aqueous synthesis of NCs,⁷ which among other improvements allows simple up-scaling. The size span of aqueous synthesized NCs is also complementary to that of the organic synthesized NCs. Very small nanoparticles could be obtained using an aqueous approach, while larger NCs are easily available from the organics-based synthesis. In terms of their potential applications in photovoltaics, it is beneficial to use both aqueous and organic synthesized NCs in order to cover a broader part of the solar spectrum, and to investigate the influence of different charge carrier and exciton confinement energies on device performances. The charge confinement in semiconductor NCs is a mixed blessing: it allows quantum size effects to be utilized, as well as increased absorption coefficients, but at the same time it limits the efficiency of current NC-based solar cells, as the confinement energy of NCs needs to be

ABSTRACT



We show that it is possible to combine several charge generation strategies in a single device structure, the performance of which benefits from all methods used. Exploiting the inherent type II heterojunction between layered structures of CdSe and CdTe colloidal quantum dots, we systematically study different ways of combining such nanocrystals of different size and surface chemistry and with different linking agents in a bilayer solar cell configuration. We demonstrate the beneficial use of two distinctly different sizes of NCs not only to improve the solar spectrum matching but also to reduce exciton binding energy, allowing their efficient dissociation at the interface. We further make use of the ligand-induced quantum-confined Stark effect in order to enhance charge generation and, hence, overall efficiency of nanocrystal-based solar cells.

KEYWORDS: nanocrystals · solar cells · ligands · quantum-confined Stark effect · type II heterojunction

overcome in order for excitons to be efficiently dissociated.⁸ Moreover, following exciton dissociation the charge carriers are localized, resulting in higher resistance. Dissociation of the excitons to free charge carriers can be promoted using a type II heterojunction between two materials, similar to the organic photovoltaics.⁹ The type II heterojunction in NC-based solar cells can be formed either between NCs layer and organic semiconducting polymers^{10–12} or between two different types of inorganic NCs, such as

* Address correspondence to nir@ee.technion.ac.il

Received for review December 15, 2011 and accepted March 5, 2012.

Published online March 05, 2012
10.1021/nn204910g

© 2012 American Chemical Society

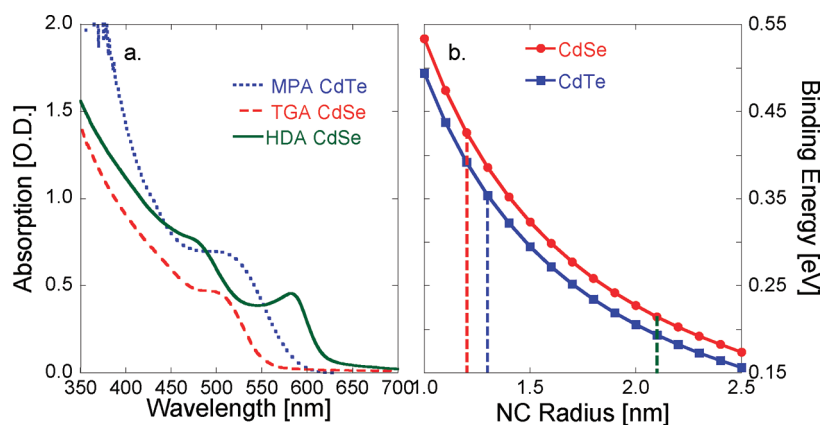


Figure 1. (a) Absorption spectra of the colloidal NCs used in this work: MPA-capped CdTe NCs (blue dotted), TGA-capped 1.2 nm radius CdSe NCs (red dashed), and HDA-capped 2.1 nm radius CdSe NCs (green solid). (b) Exciton binding energies as a function of NC radii for CdSe and CdTe (calculation is based on ref 8). The vertical dashed lines at 1.2 and 2.2 nm (CdSe) and 1.3 nm (CdTe) indicate values for our samples.

CdTe and CdSe.¹³ Recently, we demonstrated the separation of charges due to the type II alignment between CdSe and CdTe NCs by means of photoluminescence (PL) quenching¹⁴ and surface photovoltage spectroscopy.¹⁵ Talgron *et al.* compared the photoconductivity of films consisting of alternating layers of CdSe and CdTe NCs to that of single-layer NCs films and found 3-fold enhancement in photoconductivity attributed to exciton dissociation at the CdSe–CdTe interface.¹⁶ We have also shown several ligand-induced methods to overcome exciton binding energy in NC-based solar cells.^{12,17} Here we report results of a systematic study of several combinations of CdTe and CdSe NCs differing in size and their surface ligands and combine the use of cross-linking procedures¹⁸ with a ligand-induced quantum-confined Stark effect (LI-QCSE)¹⁷ in order to enhance charge generation, and hence overall efficiency, in all-NC-based type II heterojunction bi-layer solar cells.

RESULTS AND DISCUSSION

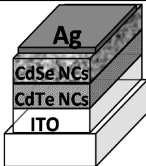
Materials' Properties. Figure 1a presents the absorption spectra of aqueous synthesized thioglycolic acid (TGA)-capped CdSe NCs (1.2 nm in radius), larger (2.1 nm in radius) hexadecylamine (HDA)-capped CdSe NCs (Nanoco Technologies), and mercaptopropionic acid (MPA)-capped CdTe NCs (1.3 nm in radius). The aqueous-based CdSe and CdTe NCs were synthesized according to previously published procedures,^{19,20} providing gram-scale products. Exciton binding energies, defined as the energy difference between the state where the electron and hole occupy a single nanocrystal and the state where they are separated on two adjacent nanocrystals, of CdSe and CdTe NCs as a function of the NCs radii have been calculated according to Leatherdale *et al.*,⁶ and the results are presented in Figure 1b. As can be seen from this graph, the binding energies are considerably larger than the few meV recorded for bulk semiconductors²¹ and cannot be overcome by

thermal energy at room temperature. In fact, these values are comparable to the recorded binding energy of organic semiconductors where a type II heterojunction is needed for charge generation.²² The binding energy of 2.1 nm CdSe NC (~ 0.21 eV) is significantly smaller than that of the 1.2 nm particles (~ 0.43 eV).

Device Structure. In order to fabricate bilayer devices that combine semiconductor NCs with different surface chemistry, we have utilized the following multistep fabrication procedure. CdTe NCs were spin coated from water solution on top of UV-ozone-treated ITO-coated glass slides, resulting in films of ~ 40 nm thickness. The films were transferred to a N_2 -filled glovebox, allowed to dry at 70 °C for 3 h *in vacuo*, and treated by soaking in ethanedithiol (EDT) dissolved in CH_3CN in order to make them insoluble in water, so that the second cycle of spin coating with the same aqueous-based solution in order to fill cracks can be carried out without destroying the film.²³ This results in a homogeneous film of ~ 60 nm thickness. Small (1.2 nm in radius) TGA-capped CdSe NCs were synthesized in water²⁰ and phase transferred to organic solvent, toluene, following a previously published protocol.²⁴ Their capping ligands were then exchanged to short conjugated methylthiophenol (MTP), and the NCs were dissolved in tetrahydrofuran (THF).¹² We then used a layer-by-layer dip-coating method with EDT as a cross-linking molecule in order to fabricate the CdSe NC top layer (~ 100 nm in thickness) of our bilayer structure. The devices were complete with thermal evaporation of the Al electrode. Table 1 illustrates the final device structure and provides details on the variations of their structure for three different types of devices realized here and discussed below.

Figure 2a illustrates the external quantum efficiency (EQE) of device 1 and compares it to the control single-layer devices of CdTe and CdSe only, which were fabricated with a similar active layer thickness of ~ 120 nm. As can be clearly seen, all the devices exhibit similar wavelength dependency (EQE shape), while the type II

TABLE 1. Device Structure of Type II Heterojunction Bilayer Solar Cells from CdTe and CdSe Nanocrystals and Summary of Structure and Performance of the Three Types of Devices Discussed

	Bi-Layer structure			EQE		I-V		
	Bottom Layer	Top Layer	Top Layer X-link	Max	J_{sc} [A/cm^2]	V_{oc} [Volt]	FF	PCE
Device 1	1.3 nm MPA CdTe NCs	1.2 nm MTP CdSe NCs	EDT	1.25%	$-2.3 \cdot 10^{-5}$	0.55	0.24	0.03%
Device 2	1.3 nm MPA CdTe NCs	2.1 nm MTP CdSe NCs	EDT	3.90%	$-9.35 \cdot 10^{-5}$	0.75	0.22	0.15%
Device 3	1.3 nm MPA CdTe NCs	2.1 nm MTP CdSe NCs	EDA	6.50%	$-1.43 \cdot 10^{-4}$	0.81	0.21	0.25%

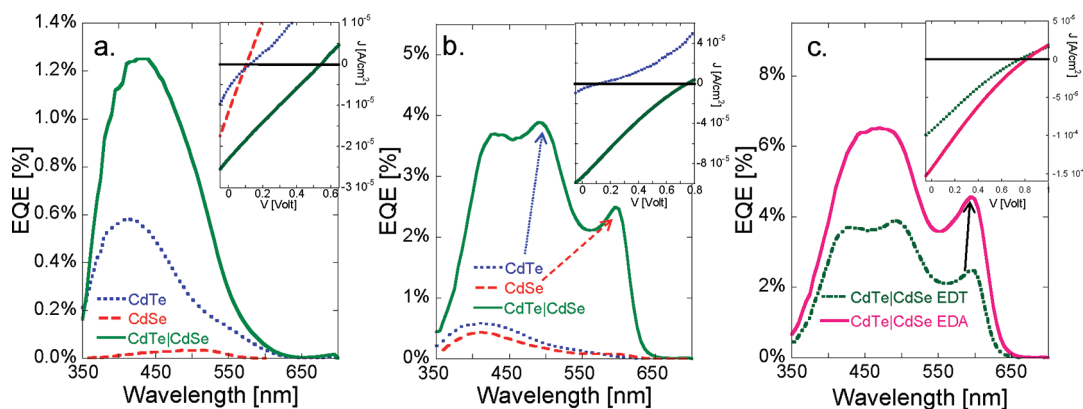


Figure 2. Performance of the reported devices: (a) External quantum efficiency of device 1 (MPA CdTe|TGA CdSe–EDT) and its control single-layer devices of CdTe and small CdSe NCs, only. (b) External quantum efficiency of device 2 (MPA CdTe|MTP CdSe–EDT) and its control single-layer devices of CdTe and large CdSe NCs, only. The arrows indicate the different layer contribution to the overall EQE. (c) External quantum efficiency of device 3 (MPA CdTe|MTP CdSe–EDA) and its control bilayer device. The oblique arrow points to the correlation between the EQE peak red-shift and EQE magnitude enhancement. Insets: current–voltage curves of these devices under standard AM1.5G 1 sun conditions.

structure device exhibits superior efficiency relative to the control devices. The inset of Figure 2a illustrates the current–voltage curves of these three devices under standard AM1.5G 1 Sun conditions. The bilayer device shows increased short circuit currents as well as higher photovoltage and fill factor. This clearly proves the charge separation due to the type II alignment in the bilayer device.

As Figure 1a shows, the absorption spectra of the 1.2 nm radius CdSe NCs and of the 1.3 nm radius CdTe NCs practically overlap. To allow the bilayer cell to absorb a larger part of the sun spectrum, it is sufficient to use a lower gap NC in only one of the layers. Figure 1b shows that the exciton binding energy of CdSe is higher than that of CdTe for any given particle size; hence, to obtain maximal gain from the increase in particle size, it is best to choose CdSe QDs as the larger size particles. In this way, both the overall absorption

spectrum is wider (~ 50 nm to the red) and the maximum binding energy is lower (*i.e.*, higher dissociation probability; see ref 25 eqs 2 and 4). To demonstrate this advantage, we have used larger (2.1 nm in radius) HDA-capped CdSe NCs with the first absorption peak at 593 nm (Figure 1a). Device 2 was fabricated in a similar manner to the previously described device 1, excluding the phase transfer step for CdSe NCs. The HDA ligands were exchanged with MTP, and the NCs were dissolved in THF. Figure 2b illustrates the EQE of this device relative to two single-layer control devices made from CdTe and MTP exchanged CdSe NCs. The bilayer device exhibits wavelength dependency, which follows the superposition of the two single-layer control devices. The overall EQE of the bilayer device 2 is higher than that of the control devices and also superior to the previous bilayer device 1 (maximum EQE approaching 4%). The inset of Figure 2b illustrates the

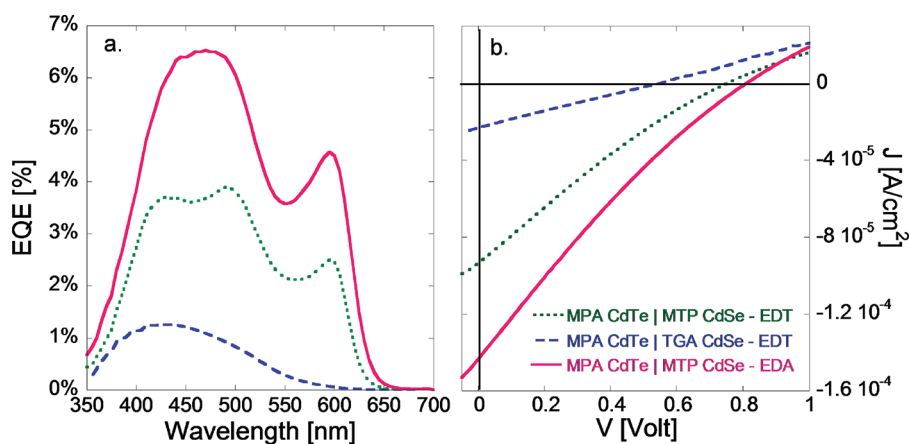


Figure 3. (a) EQE and (b) current–voltage curves of the three bilayer devices studied here, showing gradual improvement of their performance owing to proper design. The J – V curves were all measured under AM1.5G 1 sun conditions.

current–voltage curves of device 2 and compares them to the reference CdTe single-layer device. The bilayer device exhibits higher photocurrent ($9.35 \times 10^{-5} \text{ A/cm}^2$) and very high open circuit voltage of 0.75 V. We attribute this enhancement (relative to single-layer CdTe and previously discussed bilayer device 1) to the better solar spectrum coverage as well as to lower exciton binding energy of the 2.1 nm radius CdSe NCs as compared to smaller (1.2 nm) ones.

The quantum-confined Stark effect (QCSE) has been explored in detail in heterostructured semiconductor NCs,^{26,27} and we have recently suggested¹⁷ the use of a mixed capping layer around the NCs as a means to induce NC polarization due to the ligand-induced QCSE (LI-QCSE), leading to decreased exciton binding energy in CdSe NCs. As upon excitation with energies above the electronic band gap, fast relaxation to the band edges occurs,²⁸ the magnitude of the EQE is raised independently of the excitation wavelength.¹⁷ Although upon reduction in the binding energy the exciton peak would reside closer to the material band gap, the electric field influences the band gap; thus the overall energy decreases and therefore the first excitonic peak will shift to the red.²⁹ Therefore the EQE and the absorption wavelength dependency could be used as a measure of the strength of the LI-QCSE effect. We therefore fabricated yet another bilayer device (device 3), where the CdSe layer constitutes mixed-capped CdSe NCs where the ligand is MTP (thiol anchor group) and the cross-linking molecule is ethylenediamine (EDA, amine anchor group).¹⁷ This is different from the previously introduced device 2, where both the ligand (MTP) and the cross-linking molecule (EDT) bear thiol groups

anchoring to the CdSe NC surface, so that no LI-QCSE is expected. Figure 2c presents the EQE and the inset of Figure 2c shows current voltage curves of device 3, comparing them to the previously introduced bilayer device 2, which now serves as a reference sample. The mixed-ligand device exhibits enhanced charge generation (max EQE of $\sim 6.5\%$), and its current voltage curves show increased short circuit current ($1.43 \times 10^{-4} \text{ A/cm}^2$) as well as an extremely high open circuit voltage of 0.81 V. A closer look at the EQE curves in the region of the CdSe NC response reveals a 1.8 nm red-shift in the peak, which indicates that this enhancement can be indeed attributed to the LI-QCSE, as we discussed in detail in ref 17. To conclude, Figure 3 summarizes the EQE (3a) and current–voltage (3b) characteristics of devices 1–3. The gradual enhancement in device performance is clearly seen.

CONCLUSIONS

We have demonstrated the use of the inherent type II heterojunction between CdSe and CdTe NCs to design all-NC-bilayer solar cells. The possibility to employ both aqueous and organic solvent-based NCs was demonstrated. The use of CdSe NCs of larger size has been proven to be beneficial not only to achieve better solar spectrum matching but also to lower the exciton binding energy, resulting in an improved charge generation. We have further shown that even better improvement of device performance can be achieved making use of the ligand-induced quantum-confined Stark effect (LI-QCSE), showing that one can combine several methods for charge generation to arrive at better performing all-NC-based solar cells.

METHODS

Materials. Thioglycolic acid-capped CdSe NCs and mercaptopropionic acid-capped CdTe NCs were synthesized according to previous published procedures.^{19,20} HDA-capped CdSe NCs were

purchased from Nanoco Technologies. NCs sizes were determined from their absorption spectra following the method of ref 30.

Ligand Exchange. TGA-capped CdSe NCs were phase transferred to toluene following a previously published protocol,²⁴

which results in partial exchange of the TGA molecules by dodecanethiol (DDT). Both as-received HDA-capped CdSe NCs and phase-transferred TGA/DDT-capped CdSe NCs were surface modified using methylthiophenol molecules. Surface exchange was carried out under inert conditions by adding the nanocrystals to a toluene solution containing an excess of the modifying ligands (50–100-fold excess relative to the calculated original ligand content). The nanocrystals were then incubated for at least 72 h and then precipitated with methanol, separated by centrifugation, and redispersed in THF.

Device Fabrication and Characterization. CdTe NCs were spin coated from water solution on top of UV-ozone-treated patterned glass/ITO substrates (Psiotec Ltd.), resulting in films of ~40 nm thickness. The films were transferred to a N₂-filled glovebox, allowed to dry at 70 °C for 3 h *in vacuo*, and treated by soaking in ethanedithiol dissolved in CH₃CN. A second cycle of spin coating with the same aqueous-based solution was followed. The top layer of the bilayer devices was made using layer-by-layer dip coating. The substrates were dipped in a diluted solution (5 mg/mL) of CdSe NCs in THF, followed by dipping in a cross-linking molecule (EDA or EDT) in acetonitrile. Twenty dip-coating cycles were used in order to make ~100 nm thick films. The thickness of all NC-based layers were measured using a stylus profilometer (DekTak 150). The top contact was ~200 nm of Ag evaporated on top of the active layers. This electrode was deposited at <0.1 nm s⁻¹ at a pressure of ca. 1 × 10⁻⁶ mbar. The devices were then removed from the glovebox inside a nitrogen-filled sealed chamber for efficiency measurements. EQE was calculated according to $EQE(\lambda) = R(\lambda) hc/\lambda$ where λ is the incident light wavelength, h is Planck's constant, c is the speed of light, and $R(\lambda)$ is the device responsivity in [A/W] calculated by dividing the device-measured photocurrent with the incident light intensity. Devices were illuminated by mechanically chopped monochromatic light (Oriol QTH Research lamp and Cornerstone monochromator), and the photocurrent was measured using a lock-in amplifier (EG&G Instruments). The light intensity was monitored using an amplified and calibrated Si photodetector (Oriol). *I*–*V* curves were measured using a source-meter (Keithley 2400) in the dark and under 1 sun AM1.5G solar light (Sciencetech Inc. ss150 solar simulator).

Conflict of Interest: The authors declare no competing financial interest.

Acknowledgment. We acknowledge partial support of the Ollendorff Minerva Center. This work was supported by the Russell Berrie Nanotechnology Institute at the Technion–Israel Institute of Technology and by GRF project 102810 from the Research Grants Council of Hong Kong. O.S. expresses her deep gratitude to the Ministry of Absorption of the State of Israel for the Kamea Fellowship.

REFERENCES AND NOTES

- Tessler, N.; Medvedev, V.; Kazes, M.; Kan, S. H.; Banin, U. Efficient Near-Infrared Polymer Nanocrystal Light-Emitting Diodes. *Science* **2002**, *295*, 1506–1508.
- Konstantatos, G.; Howard, I.; Fischer, A.; Hoogland, S.; Clifford, J.; Klem, E.; Levina, L.; Sargent, E. H. Ultrasensitive Solution-Cast Quantum Dot Photodetectors. *Nature* **2006**, *442*, 180–183.
- Soreni-Harari, M.; Mocatta, D.; Zimin, M.; Gannot, Y.; Banin, U.; Tessler, N. Interface Modifications of InAs Quantum-Dots Solids and Their Effects on FET Performance. *Adv. Funct. Mater.* **2010**, *20*, 1005–1010.
- Hillhouse, H. W.; Beard, M. C. Solar Cells from Colloidal Nanocrystals: Fundamentals, Materials, Devices, and Economics. *Curr. Opin. Colloid Interface Sci.* **2009**, *14*, 245–259.
- Murray, C. B.; Norris, D. J.; Bawendi, M. G. Synthesis and Characterization of Nearly Monodisperse CdE (E = S, Se, Te) Semiconductor Nanocrystallites. *J. Am. Chem. Soc.* **1993**, *115*, 8706–8715.
- Reiss, P. Synthesis of Semiconductor Nanocrystals in Organic Solvents. In *Semiconductor Nanocrystal Quantum Dots—Synthesis, Assembly, Spectroscopy and Applications*; Rogach, A. L., Ed.; Springer-Verlag/Wien, 2008.
- Gaponik, N.; Talapin, D. V.; Rogach, A. L.; Hoppe, K.; Shevchenko, E. V.; Kornowski, A.; Eychmüller, A.; Weller, H. Thiol-Capping of CdTe Nanocrystals: An Alternative to Organometallic Synthetic Routes. *J. Phys. Chem. B* **2002**, *106*, 7177–7185.
- Leatherdale, C. A.; Kagan, C. R.; Morgan, N. Y.; Empedocles, S. A.; Kastner, M. A.; Bawendi, M. G. Photoconductivity in CdSe Quantum Dot Solids. *Phys. Rev. B* **2000**, *62*, 2669–2680.
- Avnon, E.; Yaacobi-Gross, N.; Ploshnik, E.; Shenhar, R.; Tessler, N. Low Cost, Nanometer Scale Nanoimprinting—Application to Organic Solar Cells Optimization. *Org. Electron.* **2011**, *12*, 1241–1246.
- Maria, A.; Cyr, P. W.; Klern, E. J. D.; Levina, L.; Sargent, E. H. Solution-Processed Infrared Photovoltaic Devices with >10% Monochromatic Internal Quantum Efficiency. *Appl. Phys. Lett.* **2005**, *87*.
- Huynh, W. U.; Dittmer, J. J.; Alivisatos, A. P. Hybrid Nanorod-Polymer Solar Cells. *Science* **2002**, *295*, 2425–2427.
- Soreni-Harari, M.; Yaacobi-Gross, N.; Steiner, D.; Aharoni, A.; Banin, U.; Millo, O.; Tessler, N. Tuning Energetic Levels in Nanocrystal Quantum Dots through Surface Manipulations. *Nano Lett.* **2008**, *8*, 678–84.
- Gur, I.; Fromer, N. A.; Geier, M. L.; Alivisatos, A. P. Air-Stable All-Inorganic Nanocrystal Solar Cells Processed from Solution. *Science* **2005**, *310*, 462–465.
- Gross, D.; Sussha, A. S.; Klar, T. A.; Da Como, E.; Rogach, A. L.; Feldmann, J. Charge Separation in Type II Tunneling Structures of Close-Packed CdTe and CdSe Nanocrystals. *Nano Lett.* **2008**, *8*, 1482–1485.
- Gross, D.; Mora-Sero, I.; Dittrich, T.; Belaidi, A.; Mauser, C.; Houtepen, A. J.; Da Como, E.; Rogach, A. L.; Feldmann, J. Charge Separation in Type II Tunneling Multilayered Structures of CdTe and CdSe Nanocrystals Directly Proven by Surface Photovoltage Spectroscopy. *J. Am. Chem. Soc.* **2010**, *132*, 5981–5983.
- Talgorn, E.; de Vries, M. A.; Siebbeles, L. D.; Houtepen, A. J. Photoconductivity Enhancement in Multilayers of CdSe and CdTe Quantum Dots. *ACS Nano* **2011**, *5*, 3552–3558.
- Yaacobi-Gross, N.; Soreni-Harari, M.; Zimin, M.; Kababya, S.; Schmidt, A.; Tessler, N. Molecular Control of Quantum-Dot Internal Electric Field and Its Application to CdSe-Based Solar Cells. *Nat. Mater.* **2011**, *10*, 974–979.
- Luther, J. M.; Law, M.; Beard, M. C.; Song, Q.; Reese, M. O.; Ellingson, R. J.; Nozik, A. J. Schottky Solar Cells Based on Colloidal Nanocrystal Films. *Nano Lett* **2008**, *8*, 3488–3492.
- Rogach, A. L.; Franzl, T.; Klar, T. A.; Feldmann, J.; Gaponik, N.; Lesnyak, V.; Shavel, A.; Eychmüller, A.; Rakovich, Y. P.; Donegan, J. F. Aqueous Synthesis of Thiol-Capped CdTe Nanocrystals: State-of-the-Art. *J. Phys. Chem. C* **2007**, *111*, 14628–14637.
- Rogach, A. L.; Kornowski, A.; Gao, M. Y.; Eychmüller, A.; Weller, H. Synthesis and Characterization of a Size Series of Extremely Small Thiol-Stabilized CdSe Nanocrystals. *J. Phys. Chem. B* **1999**, *103*, 3065–3069.
- Scholes, G. D.; Rumbles, G. Excitons in Nanoscale Systems. *Nat. Mater.* **2006**, *5*, 683–696.
- Tang, C. W. Two-Layer Organic Photovoltaic Cell. *Appl. Phys. Lett.* **1986**, *48*, 183–185.
- Koleilat, G. I.; Levina, L.; Shukla, H.; Myrskog, S. H.; Hinds, S.; Pattantyus-Abraham, A. G.; Sargent, E. H. Efficient, Stable Infrared Photovoltaics Based on Solution-Cast Colloidal Quantum Dots. *ACS Nano* **2008**, *2*, 833–840.
- Gaponik, N.; Talapin, D. V.; Rogach, A. L.; Eychmüller, A.; Weller, H. Efficient Phase Transfer of Luminescent Thiol-Capped Nanocrystals: From Water to Nonpolar Organic Solvents. *Nano Lett* **2002**, *2*, 803–806.
- Besteman, K.; Lee, J. O.; Wiertz, F. G. M.; Heering, H. A.; Dekker, C. Enzyme-Coated Carbon Nanotubes as Single-Molecule Biosensors. *Nano Lett.* **2003**, *3*, 727–730.
- Becker, K.; Lupton, J. M.; Müller, J.; Rogach, A. L.; Talapin, D. V.; Weller, H.; Feldmann, J. Electrical Control of Forster Energy Transfer. *Nat. Mater.* **2006**, *5*, 777–781.
- Müller, J.; Lupton, J. M.; Lagoudakis, P. G.; Schindler, F.; Koeppel, R.; Rogach, A. L.; Feldmann, J.; Talapin, D. V.; Weller, H. Wave Function Engineering in Elongated

- Semiconductor Nanocrystals with Heterogeneous Carrier Confinement. *Nano Lett.* **2005**, *5*, 2044–9.
28. Klimov, V. I.; McBranch, D. W. Femtosecond 1p-to-1s Electron Relaxation in Strongly Confined Semiconductor Nanocrystals. *Phys. Rev. Lett.* **1998**, *80*, 4028–4031.
 29. Miller, D. A. B.; Chemla, D. S.; Damen, T. C.; Gossard, A. C.; Wiegmann, W.; Wood, T. H.; Burrus, C. A. Band-Edge Electroabsorption in Quantum Well Structures-The Quantum-Confined Stark-Effect. *Phys. Rev. Lett.* **1984**, *53*, 2173–2176.
 30. Yu, W. W.; Qu, L. H.; Guo, W. Z.; Peng, X. G. Experimental Determination of the Extinction Coefficient of CdTe, CdSe, and CdS Nanocrystals. *Chem. Mater.* **2003**, *15*, 2854–2860.